Published in final edited form as:
Alcohol Clin Exp Res. 2010 January ; 34(1): 98–111. doi:10.1111/j.1530-0277.2009.01071.x.

Magnetic Resonance Microscopy Defines Ethanol-Induced Brain Abnormalities In Prenatal Mice: Effects Of Acute Insult On Gestational Day 7

Elizabeth A. Godin, B.S., **Shonagh K. O'Leary-Moore, Ph.D.**, **Amber A. Khan, B.S.**, **Scott E. Parnell, Ph.D.**, **Jacob J. Ament, B.S.**, **Deborah B. Dehart**, **Brice W. Johnson**, **G. Allan Johnson, Ph.D.**, **Martin A. Styner, Ph.D.**, and **Kathleen K. Sulik, Ph.D.**
Bowles Center for Alcohol Studies (EAG, SOM, AAK, SEP, JJA, DBD, KKS) and Neurodevelopmental Disorders Research Center (MAS), University of North Carolina, Chapel Hill, NC 27599

Center for *In Vivo* Microscopy, Duke University, Durham NC (BWJ, GAJ)

Abstract

Background—This magnetic resonance microscopy (MRM)-based report is the 2nd in a series designed to illustrate the spectrum of craniofacial and central nervous system (CNS) dysmorphia resulting from single- and multiple-day maternal ethanol treatment. The study described in this report examined the consequences of ethanol exposure on gestational day (GD) 7 in mice, a time in development when gastrulation and neural plate development begins; corresponding to the mid- to late 3rd week post-fertilization in humans. Acute GD 7 ethanol exposure in mice has previously been shown to result in CNS defects consistent with holoprosencephaly (HPE) and craniofacial anomalies typical of those in Fetal Alcohol Syndrome (FAS). MRM has facilitated further definition of the range of GD 7 ethanol-induced defects.

Methods—C57Bl/6J female mice were intraperitoneally administered vehicle or 2 injections of 2.9 g/kg ethanol on day 7 of pregnancy. Stage-matched control and ethanol-exposed GD 17 fetuses selected for imaging were immersion fixed in a Bouins/Prohance solution. MRM was conducted at either 7.0 Tesla (T) or 9.4 T. Resulting 29 μm isotropic spatial resolution scans were segmented and reconstructed to provide 3D images. Linear and volumetric brain measures, as well as morphological features, were compared for control and ethanol-exposed fetuses. Following MRM, selected specimens were processed for routine histology and light microscopic examination.

Results—GD 7 ethanol exposure resulted in a spectrum of median facial and forebrain deficiencies, as expected. This range of abnormalities falls within the HPE spectrum; a spectrum for which facial dysmorphology is consistent with and typically is predictive of that of the forebrain. In addition, other defects including median facial cleft, cleft palate, micrognathia, pituitary agenesis and third ventricular dilatation were identified. MRM analyses also revealed cerebral cortical dysplasia/heterotopias resulting from this acute, early insult and facilitated a subsequent focused histological investigation of these defects.

Conclusions—Individual MRM scans and 3D reconstructions of fetal mouse brains have facilitated demonstration of a broad range of GD 7 ethanol-induced morphological abnormality. These results, including the discovery of cerebral cortical heterotopias, elucidate the teratogenic potential of ethanol insult during the 3rd week of human prenatal development.

ADDRESS CORRESPONDENCE TO:, Elizabeth A. Godin, Bowles Center for Alcohol Studies, University of North Carolina, CB# 7178, Chapel Hill, NC 27599-7178, FAX: 919 966 5679, Phone: 919 966 3208, eamyers@med.unc.edu.

Keywords

Magnetic Resonance Microscopy; Fetal Alcohol Spectrum Disorder; Holoprosencephaly; Cortical Dysplasia; Leptomeningeal Heterotopia

INTRODUCTION

This is one in a series of reports (published as well as in preparation) describing developmental stage-dependent structural brain abnormalities in a mouse model of Fetal Alcohol Spectrum Disorder [FASD, the umbrella term encompassing the spectrum of prenatal ethanol exposure-induced defects, including Fetal Alcohol Syndrome (FAS)]. As for the 1st publication in this series (Parnell et al., 2009a), magnetic resonance microscopy (MRM, magnetic resonance imaging at microscopic levels) has been employed, readily allowing comprehensive structural analyses. The ethanol exposure time that is the focus of the current report is gestational day (GD) 7, a time in mouse development when gastrulation begins and neural plate formation is initiated.

That ethanol insult limited to early gastrulation stages results in a range of defects involving both the face and brain was first reported by Stockard in 1910 (Stockard, 1910). As in Stockard's investigation, which employed fish as the model system, more recently Blader and Strahl (Blader and Strahle, 1998) have reported that the ethanol-induced brain defects fall within a spectrum termed holoprosencephaly (HPE) and that in fish, there is a very narrow (3 hour) window of sensitivity during the beginning of gastrulation that is associated with this endpoint. Using a mouse model to examine ethanol teratogenesis, Sulik and Johnston (1982) also illustrated HPE resulting from acute ethanol insult during early gastrulation stages; i.e. during GD 7 in mice.

The HPE spectrum includes phenotypes ranging from the most severe, alobar form, which is characterized by a single forebrain holosphere in which there is broad communication of the lateral ventricles with each other and the third ventricle, accompanied by agenesis of the corpus callosum and olfactory bulbs; to semilobar, an intermediate form characterized by cerebral hemispheres that are most deficient rostrally and are only entirely separate through approximately their caudal half; to a least severe, lobar, form in which there is a distinct interhemispheric fissure that may or may not be interrupted anteriorly and in which the corpus callosum may be absent, hypoplastic, or normal and the olfactory bulbs may or may not be present (DeMyer and Zeman,1963). Accompanying holoprosencephalic brains are varying degrees of ocular and midfacial dysmorphology (DeMyer et al., 1964; reviewed by Muenke and Cohen, 2000; Sulik and Johnston, 1982). Examining this spectrum of defects in humans, DeMyer and colleagues (1964) noted that frequently (though not always) the face "predicts" the brain; i.e. that the severity of craniofacial and brain dysmorphology are often directly correlated. HPE is not rare. This spectrum of abnormalities is now recognized as the most commonly occurring type of birth defect, being present in as many as 1/250 human conceptuses (Matsunaga and Shiota, 1977). However, most of those affected are lost prenatally, resulting in only a 1/10,000 live birth incidence (Croen et al., 1996; reviewed in Leoncini et al., 2008; Rasmussen et al., 1996).

Study of the genesis of ethanol-induced facial and brain defects in mice (Sulik et al., 1981; Sulik and Johnston, 1982; Webster et al., 1983) led to the hypothesis that those individuals who present with the characteristic facies of full blown FAS will have brain dysmorphology falling within the HPE spectrum (Sulik and Johnston, 1982). Indeed, histological analyses of fetal mice that had FAS-like facies and had been acutely exposed to ethanol on their 7th GD have illustrated the presence of forebrain deficiencies including hypoplasia or aplasia of the

corpus callosum and septal nuclei (Schambra et al., 1990; Sulik et al., 1984). Importantly, in a non-human primate model, ethanol exposure early in pregnancy, specifically on GD 19 and 20, corresponding to the early gastrulation stage, also yielded HPE (Astley et al., 1999; Siebert et al., 1991). Features of HPE have been reported in human FAS. Indeed, in the first autopsy case-report, Jones and Smith (1975) described corpus callosum agenesis. Other autopsies revealed olfactory bulb deficiencies and pituitary abnormalities (Majewski, 1981; Peiffer et al., 1979; Shiota et al., 2007).

The advent of clinical magnetic resonance imaging (MRI) has made structural analyses of the brains in live patients with FASD possible. Initial MRI studies illustrated deficiencies in the cerebellar vermis, basal ganglia and corpus callosum in individuals with FAS (Archibald et al., 2001; Mattson et al., 1996; Riley et al., 1995). More recently, the corpus callosum has been the focus of detailed FASD imaging studies. Variability in its shape, size, and microstructure among individuals exposed to alcohol prenatally has been described (Bookstein et al., 2002; Fryer et al., 2009; Lebel et al., 2008; Ma et al., 2005; Sowell et al., 2001; Spadoni et al., 2007; Wozniak et al., 2006). While its protracted development is expected to make the corpus callosum vulnerable to teratogenic insult during many prenatal stages, when found in combination with the typical facies of FAS, it is most likely that the dysmorphology is, indeed, the result of ethanol exposure during gastrulation.

Employing a mouse FASD model, the current investigation is directed toward further defining and documenting the types and range of brain and facial defects that prenatal ethanol exposure can cause and, thus, to informing improved pre- and postnatal FASD clinical recognition and diagnosis. The acute GD7 ethanol exposure time used for this study corresponds to the mid- to late 3rd week post-fertilization in humans and is the earliest of a number of times during embryogenesis from which MRM-based data is currently being collected and compared. Since most human pregnancies remain unrecognized at this early stage, for education-based FASD prevention efforts clear illustration of the vulnerability of the brain to ethanol-mediated damage at this time is particularly important.

METHODS

Animal Maintenance

C57Bl/6J mice, purchased from The Jackson Laboratory (Bar Harbor, ME), were housed in a temperature and humidity-controlled AAALAC-approved environment. They were maintained on an *ad libitum* diet of standard laboratory chow and water. For mating, 2 females were placed with 1 male for 2 hours early in the light portion of a 12/12 hours light/dark cycle. The beginning of the breeding period in which a copulation plug was detected was defined as gestational day (GD) 0, 0 hours (h).

Maternal Treatment Paradigm

On day 7 of pregnancy, mice in the experimental group were administered two intraperitoneal doses of 25% (v/v) ethanol in lactated Ringer's solution at a dosage of 2.9 g/kg maternal body weight. The injections were given 4 h apart, with the first administered at GD 7, 0 h. Control animals were injected with an equivalent volume of lactated Ringer's solution according to the above treatment paradigm. To determine the peak blood ethanol concentration (BEC), a separate group of mice were administered ethanol, utilizing the previously described paradigm (Webster et al., 1983). Thirty minutes after the second injection, 35 μl of tail blood were obtained from each dam and analyzed using an Analox Alcohol Analyser (Model AM1, Analox Instruments USA Inc, Lunenburg, MA). All animal treatment protocols were approved by the University of North Carolina at Chapel Hill, Institutional Animal Care and Use Committee (IACUC).

Fetal Specimen Selection and Preparation

At the beginning of their 17th day of pregnancy, dams were anesthetized via CO_2 inhalation, followed by cervical dislocation. Following laparotomy, the uteri were removed and the fetuses were immediately dissected free of decidua in ice-cold phosphate buffered-saline (PBS). The GD 17 fetuses were examined for the presence of gross abnormalities. For the control group, 7 fetuses (from 4 litters) were selected for MRM scanning based on normal morphology and developmental stage-matching with the ethanol-exposed fetuses. Staging was based on degree of limb, skin, and hair follicle development (Theiler, 1989). For the ethanol group, 19 fetuses (from 8 litters) were selected for MRM scanning. As for the Parnell et al. (2009a) MRM study, selection of the ethanol-exposed fetuses was based on the presence of grossly-observable dysmorphology; an approach that is not unlike selection of children with known physical features of FAS for subsequent CNS analyses. For this investigation, all of the ethanol-exposed fetuses selected had ocular defects and among these, some had apparently normal facies, while others had obvious facial dysmorphia. To account for the entire spectrum of effect, fetuses with apparently normal, subtly affected and severely-affected facies were included. Following photography to document ocular and facial abnormalities, the fetuses were immersion fixed for 9 hours in a 20:1 solution of Bouin's fixative (Sigma-Aldrich, St. Louis, MO) containing Prohance® (Bracco Diagnostics Inc., Princeton, NJ) (Petiet et al., 2007). The specimens were then immersed in a storage solution of 200:1 PBS:Prohance in which they were held until imaged.

Magnetic Resonance Microscopy

MRM images were acquired at either 7.0Tesla (T) or 9.4T using a GE EXCITE console modified for MRM. To provide full resolution at the Nyquist frequency, a 3D rf refocused spin echo sequence (7.0T: TR = 100 ms, TE = 6.2 ms; 9.4T: TR = 75 ms, TE = 5.2 ms) with asymmetric partial Fourier sampling was used (Johnson et al., 2007). For all MRM scans acquired, the matrix size was 1024 × 512 × 512 and the FOV was 30 × 15 × 15 mm^3, which yielded an isotropic spatial resolution of 29 μm. The total scan time was approximately 4 hrs for each specimen. During scanning, specimens were immersed in fomblin, a perfluorocarbon used to limit dehydration and reduce susceptibility artifacts.

Linear Measurements

In order to ensure accurate orientation, each MRM scan was aligned in the horizontal, coronal and sagittal plane using ImageJ (Version 1.38x, NIH; http://rsbweb.nih.gov/ij/). This program was also used to obtain linear measurements. For each fetus, the following were determined: crown rump length (CRL), mid-sagittal brain length, frontothalamic distance (FTD) (excluding olfactory bulbs), bulbothalamic distance (BTD) (including olfactory bulbs), brain width (biparietal distance), third ventricle width and transverse cerebellar distance (Fig. 1a). All measurements were taken at the level of the anterior commissure, except the transverse cerebellar distance which was measured at its widest level and are reported in Table 1.

Volume Measurements

Total body (including the head) and brain volume, as well as regional brain volumes for each fetus were computed using ITK-Snap, a software program originally developed at the University of North Carolina, Chapel Hill (Yushkevich et al., 2006; www.itksnap.org). Total body volume was ascertained using the automatic segmentation feature of this program. Total brain volume was determined by adding the volumes of 17 brain regions that were each manually segmented, allowing subsequent 3D reconstruction of each region (Fig. 1c). The manually segmented regions were the right and left cortex, right and left olfactory bulb, right and left striatum, right and left hippocampus, septal region, diencephalon,

mesencephalon, pons/medulla, cerebellum, pituitary gland, lateral ventricles, third ventricle, mesencephalic (cerebral aqueduct) and fourth ventricle. In addition, for the eyes, each globe and lens was segmented. Segmentation entailed tracing each MRM slice (Fig. 1b) via a computer mouse or a pen tablet. Tracings were performed by only one individual for each selected region, for every fetus examined. Intra-rater reliability was assessed following a blind repeated segmentation of each of the selected structures in one control and one non-HPE ethanol-exposed fetus. Regional boundaries were determined based on existing fetal mouse atlases (Kaufman, 1992; Schambra et al., 1992; Schambra, 2008). Coronal, sagittal, and horizontal planes of section were used to ensure anatomical accuracy. In addition to volumetric analyses, 3D reconstructions allowed visual assessment of shape changes in ethanol-exposed versus control brains.

Routine Histology

Following imaging, each fetus was held in a 70% ethanol solution to clear the residual Bouin's fixative and to prepare the specimens for subsequent routine histological analyses. The latter was performed on selected specimens to confirm and extend MRM findings. Prior to processing, the fixed fetuses were photographed to further document facial dysmorphology. Fetal heads were removed and processed routinely for paraffin embedding using a tissue processor. Sections were cut at 10 μm, mounted on glass slides, stained with aqueous hemotoxylin and eosin (H & E), cover-slipped and viewed with a light microscope.

Statistical analyses

Group comparisons were made between stage-matched control fetuses [control] (n=7), ethanol-exposed fetuses with two distinctly separate cerebral hemispheres [non-HPE] (n=14), and ethanol-exposed fetuses with features of semilobar or alobar HPE [HPE] (n=5). Group differences among regional brain volumes, ocular measurements and linear measurements were assessed using Multivariate Analyses of Variance (MANOVAs). Crown-rump length, whole brain volume and whole body volume (including head) were analyzed using one-way ANOVAs. When applicable, post-hoc analyses were performed using Student-Newman-Keuls (SNK). An alpha value of 0.05 was maintained for all analyses.

To assess the reliability of manual segmentation of regional brain and ocular volumes, intra-rater reliability was analyzed using coefficients of variation (CV). The average CV was 3.8% (range: 0.5% – 11.8%), thus, demonstrating high reliability for manual brain segmentation.

RESULTS

General features of the study population

With a research goal of accomplishing detailed MRM-based analyses of a broad spectrum of structural brain abnormalities resulting from acute GD 7 ethanol exposure, this work employed a previously-published ethanol exposure paradigm known to yield sufficient numbers of viable fetuses having a range of effect. Consistent with previous reports, the ethanol treatment yielded peak maternal BECs (30 minutes after the second dose) averaging 440 mg/dl (range: 400 to 466 mg/dl).

The 19 ethanol-exposed GD 17 fetuses that underwent detailed MRM analyses were selected based, in part, on the presence of defects involving one or both eyes, and in part, based on facial morphology. The eye defects ranged from apparently slight microphthalmia, to iridial coloboma, to apparent anophthalmia. The facial appearance in the ethanol-exposed fetuses ranged from apparently normal to severely dysmorphic. The facial characteristics,

along with MRM-based brain findings, provided for distinction and comparison between subgroups of ethanol-exposed fetuses, as described below.

HPE

Illustrated in Fig. 2 are light micrographs of the faces and the respective brain and ventricle reconstructions of a control GD 17 fetus and of 5 ethanol-exposed fetuses that presented with varying degrees of facial dysmorphia. The facial abnormalities are consistent with those in the HPE spectrum. In the affected animals, notable features of the upper midface include a long upper lip and closely spaced nostrils. Additionally, the lower jaw is slightly to severely reduced in size (micrognathic), appearing narrow from a frontal view.

Frontal views of the reconstructed brains of the affected fetuses (Fig. 2 h–l) clearly show a spectrum of rostral union of the cerebral hemispheres along with olfactory bulb reduction to agenesis. These rostro-medial telencephalic deficiencies are consistent with HPE and grade in severity from semilobar (h) to lobar (l). From a dorsal view (Fig. 2 m–r), the varying degrees of forebrain reduction/dysmorphology are readily appreciated in the ethanol-exposed fetuses as compared to the control. Also apparent in 2 of the affected fetuses are asymmetries involving the olfactory bulbs. The animal shown in Fig. 2 h & n is more severely affected on its right, while that in i & o is more severely affected on its left. As expected, and notable in regional reconstructions and in individual MRM scans as shown in Fig. 3, are reductions in the septal region with union of the striatum across the midline. Also illustrated in Figs. 2 and 3 are the overall size reduction in the brains and the remarkably normal morphology of the brain segments caudal to the forebrain of the ethanol-exposed versus the control fetuses.

Overall, the morphology of the ventricles reflects the median forebrain deficiency in the holoprosencephalic fetuses. Most notably, rather than being continuous with the third ventricle via the narrow passages at the foramina of Monro, the lateral ventricles are broadly united with each other in the rostral midline. Accompanying the very dysmorphic lateral ventricles are third ventricles that appear relatively normal. From a dorsal view, while the ventricular space of the mesencephalon and the fourth ventricle appear normally-shaped, the aqueductal isthmus was found to be abnormally narrow in the 2 fetuses whose faces are shown in Fig. 2 e & f. The isthmus appears normal in the 3 less severely-affected fetuses in this group.

Of interest, MRM scans of all of the ethanol-exposed specimens shown in Fig. 2 revealed an aberrant tissue mass located between the base of the rostral forebrain and the nasal septum (Fig. 4 b). In some, the mass was continuous with the forebrain and in others it was not. Typically, a single mass was found to occupy a median position. However, in the animal shown in Fig. 2 c, there were two similar, more laterally-positioned masses. Subsequent routine histological coronal sections illustrate that the tissue is continuous, through the cribriform plate, with the nasal epithelium (Fig. 4 c & d; from the fetus shown in Fig. 2 d). The control counterpart is represented by olfactory nerves that extend from the nasal epithelium to the olfactory bulbs.

Cerebral Cortical Dysplasia/Heterotopia

MRM and subsequent routine histology revealed cerebral cortical dysplasia/hetertopias in ethanol-exposed fetuses whose brains were not overtly holoprosencephalic (i.e. they did not present with semilobar or alobar HPE) (Fig. 5). These cortical defects were observed in animals having facies that were apparently normal, presented with a long upper lip and severe micrognathia, foreshortened, or cleft in the midline (Fig. 5 b–e, respectively). In all of these animals, the cerebral hemispheres were completely separate and slightly widely spaced

as evidenced by the ability to visualize deep brain structures (septal region and diencephalon) from a frontal view. Additionally, both olfactory bulbs, though in some cases small and widely-spaced, were present. Initially observed in the reconstructed brain images (Fig. 5 g and j) of the fetuses shown in Fig. 5 b and e, the cortical defects present as focal protrusions on the otherwise smooth cerebral surfaces. Histological sections of these two fetuses (Fig. 5 l, q and o, t), along with sections from the other ethanol-exposed fetuses pictured in Fig. 5 (m, r and n, s) reveal relatively large and numerous, to minute and isolated irregularities in the cerebral cortex. Typically, the dysplastic/heterotopic cortical tissue was adherent to the associated leptomeninges. In the fetus with the median facial cleft (Fig. 5 e) the dysplastic cortex is localized to the medial aspect of both cerebral hemispheres, with cortical layers I through IV being involved. Subsequent to the MRM-based discovery of ethanol-induced cerebral cortical dysplasia/heterotopia, careful examination of histological sections of the brains of the fetuses with semilobar and alobar HPE revealed a small heterotopia in the frontal cortex of the most severely affected animal; the fetus shown in Fig. 2 f. No heterotopias were found in any of the control animals or any of the other ethanol-exposed fetuses.

Other dysmorphologies

A profile view (Fig. 6 b) of the fetus that is also shown in Fig. 5 d illustrates that in addition to being anophthalmic, its snout is abnormally short. MRM revealed that the nasal cavities of this fetus are very small; the turbinates are absent; and along its entire length, the nasal septum is short in the dorso-ventral direction (Fig. 6 d). Additionally, 3D reconstruction of the ventricular spaces illustrated dysmorphology involving the third ventricle presenting as excessive width and extension ventrally beyond the normal boundaries (Fig. 6 f). Both a frontal (Fig. 5 i) and a ventral view (Fig. 6 h), of the reconstructed brain of this fetus show that the olfactory bulbs are small and widely-spaced. Remarkable is the complete absence of the pituitary gland. Subsequent to MRM, examination of H & E-stained coronal histological sections of this animal revealed that the corpus callosum, while identifiable in control fetuses, was not apparent (Fig. 6 j). With the concurrent small olfactory bulbs and pituitary absence/deficiency, the dysmorphology of this brain appears to be consistent with lobar HPE.

Severe micrognathia was noted in 3 of the ethanol-exposed fetuses; those pictured in Fig. 2 b and f and in Fig. 5 c. MRM scans revealed severe micro- or aglossia in all of these animals and clefting of the secondary palate in the Fig. 2 b and 5 c fetuses. These features in the latter specimen are shown in Fig. 7, as is the reconstructed mesencephalic and fourth ventricle. Marked narrowing of the aqueductal isthmus is apparent in this fetus and is also present in 2 others (fetuses in 2 e and f; described above).

Linear and volume assessments

Due to the marked morphological differences in the brains of ethanol-exposed animals that presented with overt HPE versus the remainder that had two entirely separate cerebral hemispheres (non-HPE), measurements made for these two groups of ethanol-exposed fetuses were separately compared to controls and to each other. In spite of developmental stage-matching, there were significant differences in CRL [$F(2,22) = 5.44$, $p < 0.05$], total body volume [$F(2,23) = 4.065$, $p < 0.05$], and total brain volume [$F(2,23) = 4.51$, $p < 0.05$] between the three groups examined. Post hoc tests revealed that HPE subjects were significantly smaller than controls in terms of CRL (~9% reduction) but neither group differed from non-HPE ethanol-exposed subjects [control: 17.27 (±0.23) mm (mean ± SEM)], non-HPE: 16.38 (±0.23) mm; HPE: 15.74 (±0.31) mm]. In addition, the HPE group also had a significantly smaller total brain volume (~20% reduction) compared to controls but non-HPE ethanol-exposed animals did not differ from either HPE subjects or controls

[control: 52.86 (±2.58) mm^3, non-HPE: 47.75 (±1.52) mm^3, HPE: 42.38 (± 2.50) mm^3]. Finally, whole body volume measures for the non-HPE and HPE ethanol-exposed fetuses were decreased by 15% and 16%, respectively, as compared to controls, but SNK post-hoc tests only approached significance ($p = 0.06$) [control: 679.15 (±25.95) mm^3, non-HPE: 537.09 (±22.17) mm^3, HPE: 576.81 (± 45.93) mm^3].

Linear brain measurements are shown in Table 1. A MANOVA indicated significant group differences in linear brain measurements [$F(14,34) = 4.197$, $p < 0.05$] with significant between group effects for brain length, bulbothalamic distance (BTD), frontothalamic distance (FTD), brain width and third ventricle width (all p's < 0.05). Post hoc tests indicated that the HPE group had significantly smaller brain length, BTD and third ventricle widths compared to non-HPE subjects and controls ($p < 0.05$). FTD in HPE subjects differed only compared to controls (p's < 0.05). Brain widths were significantly smaller in HPE subjects compared to the non-HPE subjects and both ethanol-exposed groups had smaller brain widths compared to controls ($p < 0.05$). There were no differences between groups in transverse cerebellar distance ($p > 0.05$).

In spite of the overall decrease in brain volume in the HPE subjects, analyses of the regional volume measurements indicated that the overall brain volume reductions is largely the result of insult to the rostral brain structures with a remarkable sparing of more caudal regions. As expected, MANOVAs illustrated significant group differences in regional brain volumes [$F(34,16) = 3.68$, $p < 0.05$] and ocular volumes [$F(8,42) = 5.65$, $p < 0.05$] between HPE, non-HPE and control groups (Fig. 8). Significant between group effects were seen for the following brain measurements: left and right cortex, left and right olfactory bulbs, left and right striatum, septal region, diencephalon, lateral and third ventricles (all p's < 0.05). Consistent with visual inspection of the 3D reconstruction data, post hoc tests illustrated that HPE subjects had significantly smaller cortices, olfactory bulbs, striata and septal regions (which were non-existent in all HPE subjects) compared to controls and non-HPE ethanol-exposed subjects (p's < 0.05). In addition, lateral ventricles were significantly larger in HPE subjects than non-HPE and controls while the third ventricle was significantly larger in the non-HPE ethanol exposed group compared to HPE and control groups (p's < 0.05). Reductions in volumes of both the left and right globe and lens of the eyes were apparent in both ethanol exposed groups (HPE and non-HPE) compared to controls (p's < 0.05). Remarkably, despite significant dysmorphology accompanied with volumetric reductions in ethanol-exposed animals, no group differences were evident in the hippocampus, pituitary or hindbrain regions (mesencephalon, pons/medulla, cerebellum, mesencephalic and fourth ventricle) (p's > 0.05) illustrating the regional specificity of defects following exposure at this time.

In Figure 8, volumetric data is expressed to illustrate the broad range of insult. Specifically, mean control values from 7 fetuses are indicated by a black dot and the bars indicate the 95% confidence interval for the control mean. Individual data points for each ethanol-exposed subject are plotted for each region in order to convey the range of volumetric data ascertained. Values for the 5 ethanol-exposed animals with overt HPE are expressed as X's; and for all of the other ethanol-exposed animals (non-HPE, n=14) a grey circle is employed.

DISCUSSION

This report describes MRM-based discovery and documentation of structural abnormalities resulting from early gastrulation stage ethanol insult in mice. In addition to providing a 3D perspective of ethanol-induced HPE, with its range of median forebrain deficiencies, other CNS and craniofacial abnormalities were also identified. As discussed below, these findings

extend our understanding of the spectrum of ethanol-induced birth defects and of the critical periods for their induction.

It is clear that, as with other teratogens, both dosage and timing (developmental stage) dictate the consequences of prenatal ethanol exposure. Regarding the former, with the objective of identifying even the most severe of ethanol's dysmorphogenic effects, a previously-reported maternal ethanol dose high enough to yield abnormalities without substantially increasing resorption rates was selected. This dosage was somewhat higher (yielding peak maternal BECs of approx. 380 vs. 440 ± mg/dl) than utilized for an MRM-based GD 8 ethanol exposure study by Parnell et al, 2009a (the 1st publication in a series of which this is a part). On GD 8, exposure to the higher ethanol dose typically yields severe heart defects and substantial embryo lethality. As shown in previous studies that employed the same treatment paradigm as for the current investigation, peaking within 30 minutes of the last dose, the maternal BEC remains above 100 mg/dl for a total of approximately 9 hours and reaches 0 within a few more hours (Kotch et al., 1992; Webster et al., 1983). Thus, exposure to ethanol totals less than 12 hours, including a period for which the concentration is expected to be less than teratogenic. An intraperitoneal (ip) route of maternal ethanol administration was employed for both the GD 8 and the GD 7 studies. As compared to maternal dietary ethanol intake, ip administration provides interlitter outcomes that are more consistent. It is recognized that with the ip treatment, embryos may experience a higher peak ethanol concentration than occurs in the maternal blood (Clarke et al., 1985). However, it is notable that abnormalities consistent with those described herein also occur following a dietary exposure paradigm that yields maternal BECs comparable to those in the current study (Webster et al, 1983).

Regarding timing, it is clear that ethanol is teratogenic at virtually every post-implantation stage. Remarkable is that ethanol exposure occurring within a relatively narrow window in 2 hr. time-mated inbred animals can yield not only a range of defects within a single spectrum, but also defects that appear to be virtual opposites. This is exemplified by the occurrence of median forebrain and facial deficiencies typical of semilobar and alobar HPE (a narrow snout and forebrain) in some fetuses and median split face accompanied by widely spaced cerebral hemispheres and olfactory bulbs in others; all following acute insult on GD 7. Undoubtedly, the fact that in C57Bl/6J mice there is significant intra-litter variation, representing as much as 12 hours difference in developmental staging among littermates, plays an important role in this variability (Parnell et al., 2009b). HPE has been the most commonly-reported dysmorphology following GD 7 ethanol exposure in mice (Higashiyama et al., 2007, Myers et al., 2008; Schambra et al., 1990; Sulik and Johnston, 1982; Sulik et al., 1984; Webster et al., 1983), and was also observed in the current study population. GD 8 has previously been identified as the time in mouse development when median facial clefts and excessive brain width are induced by ethanol (Kotch and Sulik 1992; Parnell et al., 2009a; Webster et al., 1983), while HPE is not a typical result of GD 8 ethanol treatment. Thus, it appears that among the dysmorphic fetuses described herein, those without HPE were more developmentally advanced at the time of ethanol insult than those with HPE. While insult on each individual day of mouse development is expected to yield a specific pattern of dysmorphology, it is also expected that, due to inter- and intra- litter variability in developmental stages, there will be some overlap.

With respect to HPE, via individual scans and 3D reconstructions, MRM has made it possible to readily show the range and severity of median forebrain deficiency that occurs in the absence of overt hindbrain dysmorphology. In those cases with semilobar and alobar forms of HPE, the severity of brain effect is consistent with that of the upper midface as evidenced, to a large extent, by the proximity of the nostrils. In all of the mouse fetuses whose nostrils are too closely positioned the median portion of the upper lip is too long

(from nose to oral cavity). Notable was one fetus in which an effect on nostril positioning was subtle (if present), and that still had an unmistakably long upper lip. In this fetus the cerebrum had a complete interhemispheric fissure. It is expected that this phenotype is consistent with lobar HPE. Ongoing studies employing diffusion tensor imaging (DTI) and 3D facial analyses based on MRM reconstructions (Hammond et al., 2005) are designed to enable identification of subtle changes in facial morphology and to better define the brain fiber tracts in fetuses such as this.

The genesis of the HPE-related facial dysmorphology has previously been described as resulting from ethanol-induced loss of medial nasal prominence tissue (i.e. the progenitor of both the nasal tip and the intermaxillary segment, the latter of which becomes the philtrum of the lip and the primary palate) and subsequent overconvergence of the maxillary prominences, yielding the excessively long upper lip (Sulik and Johnston, 1983). DeMyer (1975) recognized hypoplasia of the intermaxillary segment as being pathognomonic of brain malformation; the greater the deficiency of intermaxillary tissue, the greater the likelihood of a malformed brain. In the HPE spectrum, the human face presents with an absent or indistinct philtrum accompanied by a thin (vermillion) upper lip border; a phenotype that undoubtedly results from medial nasal prominence deficiency. These facial features are also characteristic of FAS.

In addition to ethanol exposure, other environmental agents (e.g. retinoic acid, cyclopamine, cholesterol biosynthesis inhibitors) and mutations in a number of different genes including sonic hedgehog (SHH), ZIC2, SIX3, and TGIFβ can cause HPE and the associated facial abnormalities. (Cohen, 2006; Monuki, 2007; reviewed by Muenke and Cohen, 2000). Of particular note is interference with sonic hedgehog signaling (Shh-s) as a basis for these defects. Shh-s is a primary event in neural plate induction. Studies by Ahlgren and her co-workers in chicken (2002) and fish embryos (Loucks and Ahlgren, 2009) and also by Li et al. in the latter species (2007), have illustrated that ethanol interferes with this signaling. Strongly supporting this as a key mechanism underlying ethanol-induced defects is that enhancing Shh-s can diminish the teratogenesis (Loucks and Ahlgren, 2009). The prevalence of alcohol (ethanol) use and abuse and the multiple genes involved in the genesis of HPE contribute to the likelihood that via gene-environment interactions ethanol significantly factors into the high (1/250) incidence of HPE among human conceptuses (Matsunaga and Shiota, 1974).

Along with the forebrain and upper midfacial defects that characterize HPE, other defects that are associated with this spectrum were noted in this study. Micrognathia commonly occurs both in human HPE and in FASD (Ades and Sillence, 1992; Blaas et al., 2002; Cohen, 1989; Jones and Smith, 1975; Lemoine et al., 1968; Majewski, 1981; Pauli et al., 1981; 1983), and was clearly evident in a third of the 19 ethanol-exposed mouse fetuses. 3D facial analyses are expected to also identify more subtle mandibular deficiencies resulting from ethanol exposure on GD 7. Severe micrognathia was accompanied by narrowing of the cerebral aqueduct in some specimens. The latter abnormality is commonly and causally associated with hydrocephalus, a condition that co-occurs with human HPE (Barr and Cohen, 1999; Dickinson et al., 2006) and that was previously noted to result from GD 7 ethanol treatment in mice (Sulik and Johnston, 1983). Micro/aglossia and cleft palate, as seen in this study, also co-occur with HPE (Cohen, 1989; Pauli et al., 1981; 1983; Porteous et al., 1993). In part, due to the relatively long period of genesis of the secondary palate, clefting of this structure (a recognized feature of FASD) is expected to also result from ethanol insult at later developmental stages. Of these (“other”) defects, for the fetuses in this study, certainly aqueductal stenosis, and probably cleft palate would not have been readily recognized without MRM.

Also with MRM, tissue that appears to correspond to misplaced olfactory nerves was found in the overtly holoprosencephalic animals. Normally, the olfactory nerves should project from the nasal epithelium, through the cribriform plate, to synapse in the olfactory bulbs. In the absence of olfactory bulbs, these nerves still extend upward, but lacking a target, form an intracranial mass that remains unattached to the brain. Recent analyses of holoprosencephalic mouse fetuses whose defects resulted from Shh-inhibition via *in utero* exposure to a potent cyclopamine analog revealed comparable olfactory nerve masses (R.J. Lipinski, personal communication).

Two of the ethanol-exposed fetuses in this study have small, widely spaced olfactory bulbs. Of these, one is anophthalmic and has an enlarged third ventricle (indicating hypothalamic deficiency), no pituitary, apparent absence of the corpus callosum, and markedly small/stenotic nasal cavities. The other has a median facial cleft. The collection of defects in these mice is consistent with the following recognized human syndromes/associations: 1) median cleft face syndrome; a condition for which agenesis of the corpus callosum and anomalies of the pituitary gland have been reported (DeMyer, 1967), 2) septo-optic dysplasia; a syndrome characterized by absence of the septum pellucidum, pituitary hormone deficiency, and optic nerve hypoplasia; features of which a clinical report by Coulter et al. (1993) attributed to prenatal ethanol exposure, and 3) CHARGE association which includes nasal cavity narrowing, growth and mental retardation, along with a variety of structural brain abnormalities including absence/hypoplasia of the olfactory bulbs and tracts, dysgenesis / hypoplasia of the frontal lobes and optic nerves, and agenesis of the corpus callosum and septum pellucidum. CHARGE association was highlighted in the Parnell et al. (2009a) report as resulting from GD 8 ethanol exposure in mice. Indeed, although each has its own key features, there is significant overlap between HPE and these 3 clinical conditions (Bomelburg et al., 1987; de Toni et al., 1985; Fitz, 1994; Lin et al., 1990; Polizzi et al., 2005). This is also true for the dysmorphology resulting from GD 7 versus GD 8 ethanol exposure in mice.

The MRM-based discovery of cerebral cortical dysplasia/heterotopias resulting from acute GD 7 ethanol exposure is novel and is expected to be of significant clinical importance. Nearly 35 years ago the first autopsy report by Jones and Smith (1975) of a newborn with FAS described a large heterotopia encompassing the left cerebral hemisphere. Under this mass of tissue, the cortex was thin and disorganized and the lateral ventricles were enlarged. In more recent studies of rodent FASD models, one of which was conducted utilizing cultured GD17 fetal rat cortical slices (Mooney et al., 2004) and one which employed maternal dietary ethanol exposure on days 10 through 21 in the rat (Komatsu et al., 2001; Sakata-Haga et al., 2004), cortical heterotopias have also been found. The cortical defects noted in the current study ranged from extremely small and isolated, to involving the medial aspect of both cerebral hemispheres. In most cases, the morphology is consistent with leptomeningeal heterotopia, though a more accurate descriptor for the most extensive defects is probably cortical dysplasia. Cortical heterotopias are generally considered as resulting from neuronal migration errors (Verotti et al., 2009). It is remarkable that they can result from an acute teratogenic insult occurring as early as the time of neural plate induction.

The presence of cortical heterotopias is highly correlated with seizure activity. Indeed, Verroti et al. (2009) state that “neuronal migration disorders are considered to be one of the most significant causes of neurological and developmental disabilities and epileptic seizures in childhood”. Among individuals with FAS the prevalence of epilepsy is higher than in the general population (1%), with estimates varying from 3–21% (Dorris, 1989; Ioffe and Chernick, 1990; Jones et al., 1973; Majewski, 1981; Marcus, 1987; Murray-Lyon, 1985; Olegard et al., 1979; O’Malley and Barr, 1998; Streissguth et al., 1978). Work directed

toward identifying pathologic changes that may underlie alcohol-induced seizure threshold reduction has shown an association with hippocampal abnormalities induced during the human 3rd trimester equivalent (Bonthius et al., 2001 a,b). These studies employed a rat FASD model in which both behavioral and electrographic seizure thresholds were examined. Similar testing of postnatal animals following acute ethanol exposure during early gastrulation is needed.

Linear and volume measurements made in this study from MRM scans and 3D reconstructions are consistent with the visually-assessed dysmorphology. Notable in the ethanol-exposed animals are reduced frontothalamic and brain width measures and lateral ventricular enlargement; features that can be readily assessed in human fetal ultrasounds. Work by Kfir et al. (2009) showing that both 2nd and 3rd trimester ultrasound can detect frontothalamic reductions in the fetuses of moderate to heavy alcohol users, is consistent with the mouse data (Sulik et al., 2009). Together, the human and experimental studies illustrate the diagnostic potential of early (prenatal) forebrain measures.

In conclusion, this work contributes significantly to defining the CNS dysmorphology that results from ethanol insult at times corresponding to the middle through the end of the 3rd week of human development. Individual MRM scans and 3D reconstructions of fetal mouse brains have facilitated this effort, allowing documentation and discovery of ethanol-induced CNS defects and appreciation of their relationship to co-occurring facial abnormalities. These results promise to aid in clinical recognition, diagnosis, and prevention of FASD.

Acknowledgments

SOURCES OF SUPPORT: This work was supported by NIH/NIAAA grants AA007573, AA11605, AA017124; NCRR/NCI grants P41 05959 and U24 CA092656; and the UNC Neurodevelopmental Disorders Research Center HD 03110; and was done in conjunction with the Collaborative Initiative on Fetal Alcohol Spectrum Disorders (CIFASD). Additional information about the CIFASD can be found at www.cifasd.org.

REFERENCES

Ades LC, Sillence DO. Agnathia-holoprosencephaly with tetramelia. Clin Dysmorphol. 1992; 1(3): 182–184. [PubMed: 1342869]

Ahlgren SC, Thakur V, Bronner-Fraser M. Sonic hedgehog rescues cranial neural crest from cell death induced by ethanol exposure. Proc Natl Acad Sci U S A. 2002; 99(16):10476–10481. [PubMed: 12140368]

Archibald SL, Fennema-Notestine C, Gamst A, Riley EP, Mattson SN, Jernigan TL. Brain dysmorphology in individuals with severe prenatal alcohol exposure. Dev Med Child Neurol. 2001; 43(3):148–154. [PubMed: 11263683]

Astley SJ, Magnuson SI, Omnell LM, Clarren SK. Fetal alcohol syndrome: changes in craniofacial form with age, cognition, and timing of ethanol exposure in the macaque. Teratology. 1999; 59(3): 163–172. [PubMed: 10194807]

Barr M Jr, Cohen MM Jr. Holoprosencephaly survival and performance. Am J Med Genet. 1999; 89(2):116–120. [PubMed: 10559767]

Blaas HG, Eriksson AG, Salvesen KA, Isaksen CV, Christensen B, Mollerlokken G, Eik-Nes SH. Brains and faces in holoprosencephaly: pre- and postnatal description of 30 cases. Ultrasound Obstet Gynecol. 2002; 19(1):24–38. [PubMed: 11851965]

Blader P, Strahle U. Ethanol impairs migration of the prechordal plate in the zebrafish embryo. Dev Biol. 1998; 201(2):185–201. [PubMed: 9740658]

Bomelburg T, Lenz W, Eusterbrock T. Median cleft face syndrome in association with hydrocephalus, agenesis of the corpus callosum, holoprosencephaly and choanal atresia. Eur J Pediatr. 1987; 146(3):301–302. [PubMed: 3595651]

Bonthius DJ, Woodhouse J, Bonthius NE, Taggard DA, Lothman EW. Reduced seizure threshold and hippocampal cell loss in rats exposed to alcohol during the brain growth spurt. Alcohol Clin Exp Res. 2001a; 25(1):70–82. [PubMed: 11198717]

Bonthius DJ, Pantazis NJ, Karacay B, Bonthius NE, Taggard Da, Lothman EW. Alcohol exposure during the brain growth spurt promotes hippocampal seizures, rapid kindling, and spreading depression. Alcohol Clin Exp Res. 2001b; 25(5):734–745. [PubMed: 11371723]

Bookstein FL, Sampson PD, Connor PD, Streissguth AP. Midline corpus callosum is a neuroanatomical focus of fetal alcohol damage. Anat Rec. 2002; 269(3):162–174. [PubMed: 12124903]

Clarke DW, Steenaart NA, Breedon TH, Brien JF. Differential pharmacokinetics for oral and intraperitoneal administration of ethanol to the pregnant guinea pig. Can J Physiol Pharmacol. 1985; 63(2):169–172. [PubMed: 3986701]

Cohen MM Jr. Perspectives on holoprosencephaly: Part I. Epidemiology, genetics, and syndromology. Teratology. 1989; 40(3):211–235. [PubMed: 2688166]

Cohen MM Jr. Holoprosencephaly: clinical, anatomic, and molecular dimensions. Birth Defects Res A Clin Mol Teratol. 2006; 76(9):658–673. [PubMed: 17001700]

Coulter CL, Leech RW, Schaefer GB, Scheithauer BW, Brumback RA. Midline cerebral dysgenesis, dysfunction of the hypothalamic-pituitary axis, and fetal alcohol effects. Arch Neurol. 1993; 50(7): 771–775. [PubMed: 8323485]

Croen LA, Shaw GM, Lammer EJ. Holoprosencephaly: epidemiologic and clinical characteristics of a California population. Am J Med Genet. 1996; 64(3):465–472. [PubMed: 8862623]

DeMyer W, Zeman W. Alobar holoprosencephaly (arhinencephaly) with median cleft lip and palate: clinical, electroencephalographic and nosologic considerations. Confin Neurol. 1963; 23:1–36. [PubMed: 14026941]

DeMyer W, Zeman W, Palmer CG. The Face Predicts the Brain: Diagnostic Significance of Median Facial Anomalies for Holoprosencephaly (Arhinencephaly). Pediatrics. 1964; 34:256–263. [PubMed: 14211086]

DeMyer W. The median cleft face syndrome. Differential diagnosis of cranium bifidum occultum, hypertelorism, and median cleft nose, lip, and palate. Neurology. 1967; 17(10):961–971. [PubMed: 6069608]

DeMyer W. Median facial malformations and their implications for brain malformations. Birth Defects Orig Artic Ser. 1975; 11(7):155–181. [PubMed: 764897]

Dickinson BP, Spoon DB, Cordray TL, Lazareff J, Wasson K, Bradley JP. Correction of massive hydrocephalus and brain wound in holoprosencephaly. J Craniofac Surg. 2006; 17(4):707–713. [PubMed: 16877920]

Dorris, M. The Broken Cord. New York: Harper and Row Publishers Inc.; 1989.

Fitz CR. Holoprosencephaly and septo-optic dysplasia. Neuroimaging Clin N Am. 1994; 4(2):263–281. [PubMed: 8081628]

Fryer SL, Schweinsburg BC, Bjorkquist OA, Frank LR, Mattson SN, Spadoni AD, Riley EP. Characterization of white matter microstructure in fetal alcohol spectrum disorders. Alcohol Clin Exp Res. 2009; 33(3):514–521. [PubMed: 19120066]

Hammond P, Hutton TJ, Allanson JE, Buxton B, Campbell LE, Clayton-Smith J, Donnai D, Karmiloff-Smith A, Metcalfe K, Murphy KC, Patton M, Pober B, Prescott K, Scambler P, Shaw A, Smith AC, Stevens AF, Temple IK, Hennekam R, Tassabehji M. Discriminating power of localized three-dimensional facial morphology. Am J Hum Genet. 2005; 77(6):999–1010. [PubMed: 16380911]

Higashiyama D, Saitsu H, Komada M, Takigawa T, Ishibashi M, Shiota K. Sequential developmental changes in holoprosencephalic mouse embryos exposed to ethanol during the gastrulation period. Birth Defects Res A Clin Mol Teratol. 2007; 79(7):513–523. [PubMed: 17393481]

Ioffe S, Chernick V. Prediction of subsequent motor and mental retardation in newborn infants exposed to alcohol in utero by computerized EEG analysis. Neuropediatrics. 1990; 21(1):11–17. [PubMed: 2314553]

Johnson GA, Ali-Sharief A, Badea A, Brandenburg J, Cofer G, Fubara B, Gewalt S, Hedlund LW, Upchurch L. High-throughput morphologic phenotyping of the mouse brain with magnetic resonance histology. Neuroimage. 2007; 37(1):82–89. [PubMed: 17574443]

Jones KL, Smith DW, Ulleland CN, Streissguth P. Pattern of malformation in offspring of chronic alcoholic mothers. Lancet. 1973; 1(7815):1267–1271. [PubMed: 4126070]

Jones KL, Smith DW. The fetal alcohol syndrome. Teratology. 1975; 12(1):1–10. [PubMed: 1162620]

Kaufman, MH. The Atlas of Mouse Development. San Diego: Academic Press; 1992.

Kfir M, Yevtushok L, Onishchenko S, Wertelecki W, Bakhireva L, Chambers CD, Jones KL, Hull AD. Can prenatal ultrasound detect the effects of in-utero alcohol exposure? A pilot study. Ultrasound Obstet Gynecol. 2009; 33(6):683–689. [PubMed: 19444822]

Komatsu S, Sakata-Haga H, Sawada K, Hisano S, Fukui Y. Prenatal exposure to ethanol induces leptomeningeal heterotopia in the cerebral cortex of the rat fetus. Acta Neuropathol. 2001; 101(1): 22–26. [PubMed: 11194937]

Komatsu S, Sakata-Haga H, Sawada K, Hisano S, Fukui Y. Prenatal exposure to ethanol induces leptomeningeal heterotopia in the cerebral cortex of the rat fetus. Acta Neuropathol. 2001; 101(1): 22–26. [PubMed: 11194937]

Kotch LE, Dehart DB, Alles AJ, Chernoff N, Sulik KK. Pathogenesis of ethanol-induced limb reduction defects in mice. Teratology. 1992; 46(4):323–332. [PubMed: 1412063]

Kotch LE, Sulik KK. Experimental fetal alcohol syndrome: proposed pathogenic basis for a variety of associated facial and brain anomalies. Am J Med Genet. 1992; 44(2):168–176. [PubMed: 1456286]

Lebel C, Rasmussen C, Wyper K, Walker L, Andrew G, Yager J, Beaulieu C. Brain diffusion abnormalities in children with fetal alcohol spectrum disorder. Alcohol Clin Exp Res. 2008; 32(10):1732–1740. [PubMed: 18671811]

Lemoine P, Harousseau H, Borteyru JP, Menuet J. Les enfants de parents alcooliques: anomalies observees. Quest Med. 1968; 25:476–482.

Leoncini E, Baranello G, Orioli IM, Anneren G, Bakker M, Bianchi F, Bower C, Canfield MA, Castilla EE, Cocchi G, Correa A, De Vigan C, Doray B, Feldkamp ML, Gatt M, Irgens LM, Lowry RB, Maraschini A, Mc Donnell R, Morgan M, Mutchinick O, Poetzsch S, Riley M, Ritvanen A, Gnansia ER, Scarano G, Sipek A, Tenconi R, Mastroiacovo P. Frequency of holoprosencephaly in the International Clearinghouse Birth Defects Surveillance Systems: searching for population variations. Birth Defects Res A Clin Mol Teratol. 2008; 82(8):585–591. [PubMed: 18566978]

Li YX, Yang HT, Zdanowicz M, Sicklick JK, Qi Y, Camp TJ, Diehl AM. Fetal alcohol exposure impairs Hedgehog cholesterol modification and signaling. Lab Invest. 2007; 87(3):231–240. [PubMed: 17237799]

Lin AE, Siebert JR, Graham JM Jr. Central nervous system malformations in the CHARGE association. Am J Med Genet. 1990; 37(3):304–310. [PubMed: 2260555]

Loucks EJ, Ahlgren SC. Deciphering the role of Shh signaling in axial defects produced by ethanol exposure. Birth Defects Res A Clin Mol Teratol. 2009; 85(6):556–567. [PubMed: 19235835]

Ma X, Coles CD, Lynch ME, Laconte SM, Zurkiya O, Wang D, Hu X. Evaluation of corpus callosum anisotropy in young adults with fetal alcohol syndrome according to diffusion tensor imaging. Alcohol Clin Exp Res. 2005; 29(7):1214–1222. [PubMed: 16046877]

Majewski F. Alcohol embryopathy: some facts and speculations about pathogenesis. Neurobehav Toxicol Teratol. 1981; 3(2):129–144. [PubMed: 7195989]

Marcus JC. Neurological findings in the fetal alcohol syndrome. Neuropediatrics. 1987; 18(3):158–160. [PubMed: 3683756]

Matsunaga E, Shiota K. Holoprosencephaly in human embryos: epidemiologic studies of 150 cases. Teratology. 1977; 16(3):261–272. [PubMed: 594909]

Mattson SN, Riley EP, Sowell ER, Jernigan TL, Sobel DF, Jones KL. A decrease in the size of the basal ganglia in children with fetal alcohol syndrome. Alcohol Clin Exp Res. 1996; 20(6):1088–1093. [PubMed: 8892532]

Monuki ES. The morphogen signaling network in forebrain development and holoprosencephaly. J Neuropathol Exp Neurol. 2007; 66(7):566–575. [PubMed: 17620982]

Mooney SM, Siegenthaler JA, Miller MW. Ethanol induces heterotopias in organotypic cultures of rat cerebral cortex. Cereb Cortex. 2004; 14(10):1071–1080. [PubMed: 15166098]

Muenke M, Cohen MM Jr. Genetic approaches to understanding brain development: holoprosencephaly as a model. Ment Retard Dev Disabil Res Rev. 2000; 6(1):15–21. [PubMed: 10899793]

Murray-Lyon IM. Alcohol and foetal damage. Alcohol Alcohol. 1985; 20(2):185–188. [PubMed: 4052154]

Myers EA, Parnell SE, Dehart DB, Johnson GA, Sulik KK. Analysis of Ethanol-Induced Abnormalities in the Medial Forebrain of Fetal Mice. Toxicologist CD - An official J Soc Toxicol. 2008; 102:1530.

O'Malley KD, Barr H. Fetal alcohol syndrome and seizure disorder. Can J Psychiatry. 1998; 43(10): 1051. [PubMed: 9868573]

Olegard R, Sabel KG, Aronsson M, Sandin B, Johansson PR, Carlsson C, Kyllerman M, Iversen K, Hrbek A. Effects on the child of alcohol abuse during pregnancy. Retrospective and prospective studies. Acta Paediatr Scand Suppl. 1979; 275:112–121. [PubMed: 291283]

Parnell SE, O'Leary-Moore SK, Godin EA, Dehart DB, Johnson BW, Allan Johnson G, Styner MA, Sulik KK. Magnetic Resonance Microscopy Defines Ethanol-Induced Brain Abnormalities in Prenatal Mice: Effects of Acute Insult on Gestational Day 8. Alcohol Clin Exp Res. 2009a; 33(6): 1001–1011. [PubMed: 19302087]

Parnell SE, Dehart DB, Zhou FC, Sulik KK. Sub-strain-dependent variability in susceptibility to ethanol-induced teratogenesis. Alcohol Clin Exp Res. 2009b; 33(S1):132A.

Pauli RM, Graham JM Jr, Barr M Jr. Agnathia, situs inversus, and associated malformations. Teratology. 1981; 23(1):85–93. [PubMed: 7245093]

Pauli RM, Pettersen JC, Arya S, Gilbert EF. Familial agnathia-holoprosencephaly. Am J Med Genet. 1983; 14(4):677–698. [PubMed: 6846401]

Peiffer J, Majewski F, Fischbach H, Bierich JR, Volk B. Alcohol embryo- and fetopathy. Neuropathology of 3 children and 3 fetuses. J Neurol Sci. 1979; 41(2):125–137. [PubMed: 438847]

Petiet A, Hedlund L, Johnson GA. Staining methods for magnetic resonance microscopy of the rat fetus. J Magn Reson Imaging. 2007; 25(6):1192–1198. [PubMed: 17520739]

Polizzi A, Pavone P, Iannetti P, Gambardella A, Ruggieri M. CNS findings in three cases of septo-optic dysplasia, including one with semilobar holoprosencephaly. Am J Med Genet A. 2005; 136A(4):357. [PubMed: 15942946]

Porteous ME, Wright C, Smith D, Burn J. Agnathia-holoprosencephaly: a new recessive syndrome? Clin Dysmorphol. 1993; 2(2):161–164. [PubMed: 8281280]

Rasmussen SA, Moore CA, Khoury MJ, Cordero JF. Descriptive epidemiology of holoprosencephaly and arhinencephaly in metropolitan Atlanta, 1968–1992. Am J Med Genet. 1996; 66(3):320–333. [PubMed: 8985495]

Riley EP, Mattson SN, Sowell ER, Jernigan TL, Sobel DF, Jones KL. Abnormalities of the corpus callosum in children prenatally exposed to alcohol. Alcohol Clin Exp Res. 1995; 19(5):1198–1202. [PubMed: 8561290]

Sakata-Haga H, Sawada K, Ohnishi T, Fukui Y. Hydrocephalus following prenatal exposure to ethanol. Acta Neuropathol. 2004; 108(5):393–398. [PubMed: 15365720]

Schambra UB, Lauder JM, Petrusz P, Sulik KK. Development of neurotransmitter systems in the mouse embryo following acute ethanol exposure: a histological and immunocytochemical study. Int J Dev Neurosci. 1990; 8(5):507–522. [PubMed: 1980786]

Schambra, UB.; Lauder, JM.; Silver, J. Atlas of Prenatal Mouse Brain. San Diego: Academic Press; 1992.

Schambra, UB. Prenatal Mouse Brain Atlas. New York: Springer Science + Business Media; 2008.

Shiota K, Yamada S, Komada M, Ishibashi M. Embryogenesis of holoprosencephaly. Am J Med Genet A. 2007; 143A(24):3079–3087. [PubMed: 17963261]

Siebert JR, Astley SJ, Clarren SK. Holoprosencephaly in a fetal macaque (Macaca nemestrina) following weekly exposure to ethanol. Teratology. 1991; 44(1):29–36. [PubMed: 1957260]

Sowell ER, Mattson SN, Thompson PM, Jernigan TL, Riley EP, Toga AW. Mapping callosal morphology and cognitive correlates: effects of heavy prenatal alcohol exposure. Neurology. 2001; 57(2):235–244. [PubMed: 11468307]

Spadoni AD, McGee CL, Fryer SL, Riley EP. Neuroimaging and fetal alcohol spectrum disorders. Neurosci Biobehav Rev. 2007; 31(2):239–245. [PubMed: 17097730]

Stockard CR. The influence of alcohol and other anaesthetics on embryonic development. Am J Anat. 1910; 10:369–392.

Streissguth AP, Herman CS, Smith DW. Intelligence, behavior, and dysmorphogenesis in the fetal alcohol syndrome: a report on 20 patients. J Pediatr. 1978; 92(3):363–367. [PubMed: 632974]

Sulik KK, Johnston MC. Embryonic origin of holoprosencephaly: interrelationship of the developing brain and face. Scan Electron Microsc. 1982; (Pt 1):309–322. [PubMed: 7167750]

Sulik KK, Johnston MC. Sequence of developmental alterations following acute ethanol exposure in mice: craniofacial features of the fetal alcohol syndrome. Am J Anat. 1983; 166(3):257–269. [PubMed: 6846205]

Sulik KK, Johnston MC, Webb MA. Fetal alcohol syndrome: embryogenesis in a mouse model. Science. 1981; 214(4523):936–938. [PubMed: 6795717]

Sulik KK, Lauder JM, Dehart DB. Brain Malformations in Prenatal Mice Following Acute Maternal Ethanol Administration. Int J Dev Neurosci. 1984; 2(3):203–214.

Sulik KK, O'Leary-Moore SK, Parnell SE, Myers EA, Dehart DB, Johnson GA, Chambers CD, Hull AD. High resolution magnetic resonance imaging of alcohol-exposed fetal mice confirms and informs human prenatal ultrasound studies. Proceedings of the Greenwood Genetic Center. 2009; 28 *in press*.

Theiler, K. The House Mouse: Atlas of Embryonic Development. New York: Springer-Verlag; 1989.

de Toni T, Lazzaroni-Fossati F, Gastaldi R, Taccone A, Pesce F, Piccotti E, Balzarini C, Tarateta A. Median cleft face syndrome associated with holoprosencephaly. Description of a case. Minerva Pediatr. 1985; 37(21–22):875–882. [PubMed: 4094605]

Verrotti A, Spalice A, Ursitti F, Papetti L, Mariani R, Castronovo A, Mastrangelo M, Iannetti P. New trends in neuronal migration disorders. Eur J Paediatr Neurol. 2009 *In press*.

Webster WS, Walsh DA, McEwen SE, Lipson AH. Some teratogenic properties of ethanol and acetaldehyde in C57BL/6J mice: implications for the study of the fetal alcohol syndrome. Teratology. 1983; 27(2):231–243. [PubMed: 6867945]

Wozniak JR, Mueller BA, Chang PN, Muetzel RL, Caros L, Lim KO. Diffusion tensor imaging in children with fetal alcohol spectrum disorders. Alcohol Clin Exp Res. 2006; 30(10):1799–1806. [PubMed: 17010147]

Yushkevich PA, Piven J, Hazlett HC, Smith RG, Ho S, Gee JC, Gerig G. User-guided 3D active contour segmentation of anatomical structures: significantly improved efficiency and reliability. Neuroimage. 2006; 31(3):1116–1128. [PubMed: 16545965]

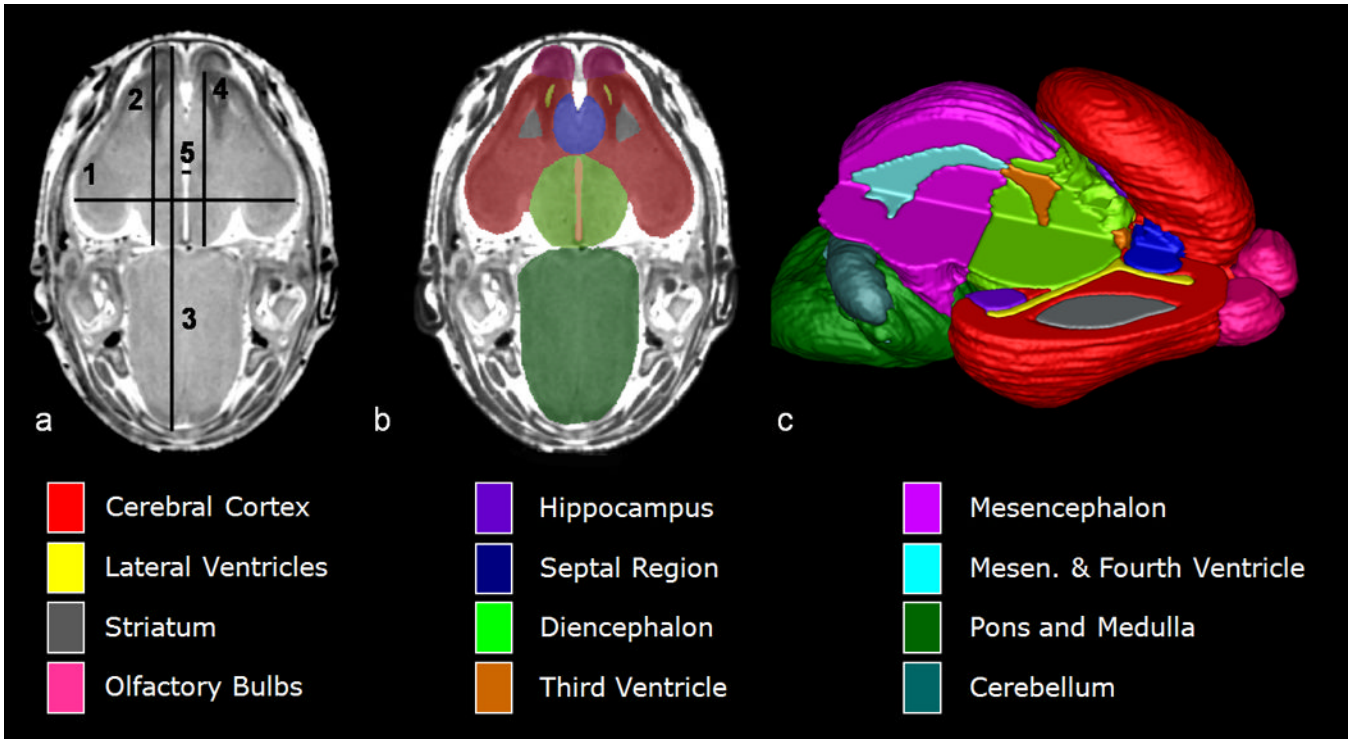

Figure 1.
MRM scans of GD 17 mouse fetuses allow for linear measurements, regional segmentation, and 3D reconstruction. Illustrated in (a) is a horizontal scan with lines depicting sites of linear measurement as follows: brain width (biparietal distance), line 1; bulbothalamic distance, line 2; mid-sagittal brain length, line 3; frontothalamic distance, line 4; third ventricle width, line 5. [Cerebellar width (transverse cerebellar distance, not included) was measured at its greatest dimension.] Manual segmentation, as depicted by the color-coded regions in (b) allowed for subsequent 3D reconstruction (c) and analyses of selected brain regions. In (c), the upper right quadrant of the brain has been removed to allow for visualization of the interior structures. Color-codes for the segmented brain regions shown are at the bottom of the Figure. Other regions that were also examined for each of the animals in this study, but are not shown in this illustration, are the pituitary and the ocular globe and lens of each eye. (modified from Figs. 1 & 2, Parnell et al, 2009a)

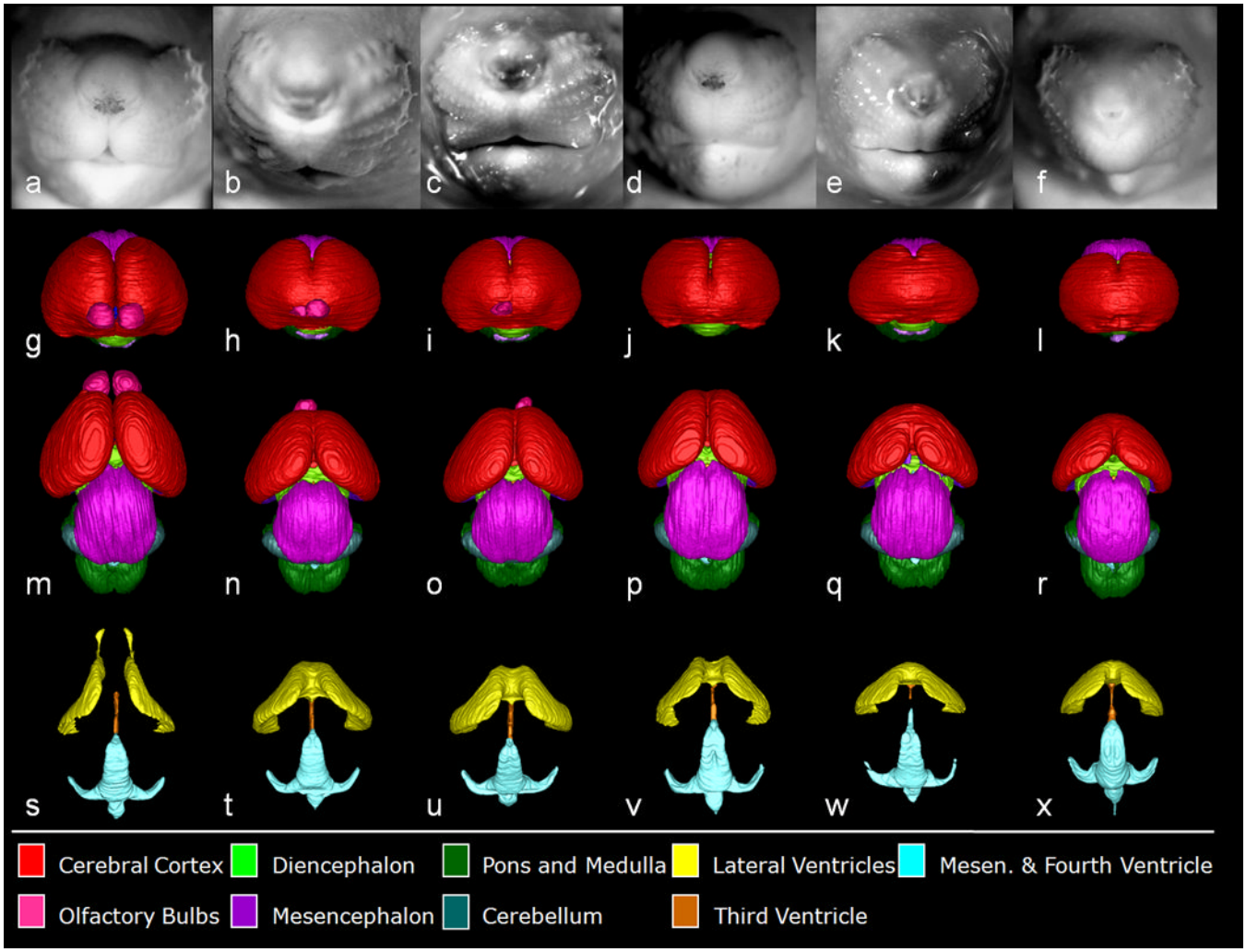

Figure 2.

Shown are the face and reconstructed brain of a control GD 17 fetal mouse along with the faces and brains of ethanol-exposed fetuses having semilobar and alobar holoprosencephaly (HPE). As compared to the control face (a), those fetuses with HPE (b–f) have varying degrees of midfacial abnormality; each presenting with a long (from nose to mouth) upper lip, a small nose with closely-set nostrils, and micrognathia (narrow, pointed chin), the latter of which is severe in the specimens shown in (b) and (f). Segmented MRM scans of control (g, m, s) and ethanol-exposed fetuses (h–l, n–r, t–x) were reconstructed to yield whole brain (frontal view, g–l; dorsal view, m–r) and ventricular system (s–x) images. Notable forebrain abnormalities include varying degrees of olfactory bulb deficiency and rostral union of the cerebral hemispheres, accompanied by dysmorphic lateral ventricles. From a dorsal view, the mid- and hindbrain and their ventricles appear relatively normal in all of the affected fetuses. Color codes for the segmented brain regions are shown at the bottom of the Figure.

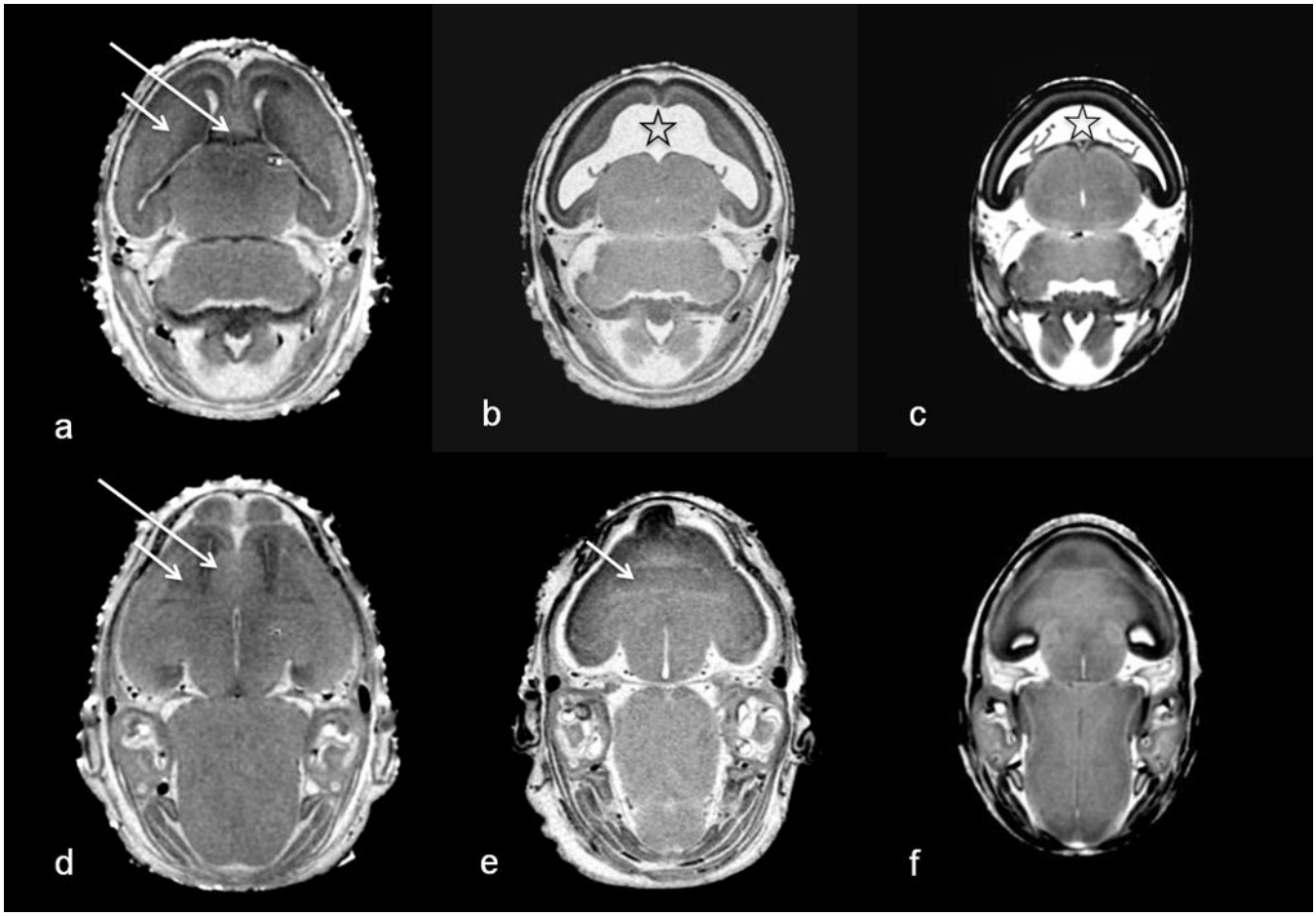

Figure 3.

Horizontal MRM scans at 2 different levels through a control (a. d) and 2 affected fetuses (b, e with semilobar HPE & c, f with alobar HPE; shown in Fig. 2 b, f, respectively) illustrate rostro-median tissue loss. The septal region (long arrow), which is apparent in the rostral midline of the control, is absent in the affected fetuses. In the more mildly affected fetus (b, e), the striatal tissue (short arrow) can be defined and, in the absence of the septal region, is united across the midline. In the more severely affected fetus (c, f), MRM does not allow clear identification of the striatal boundaries. Notable in both affected fetuses is the vastly enlarged and rostro-medially fused lateral ventricles (✭).

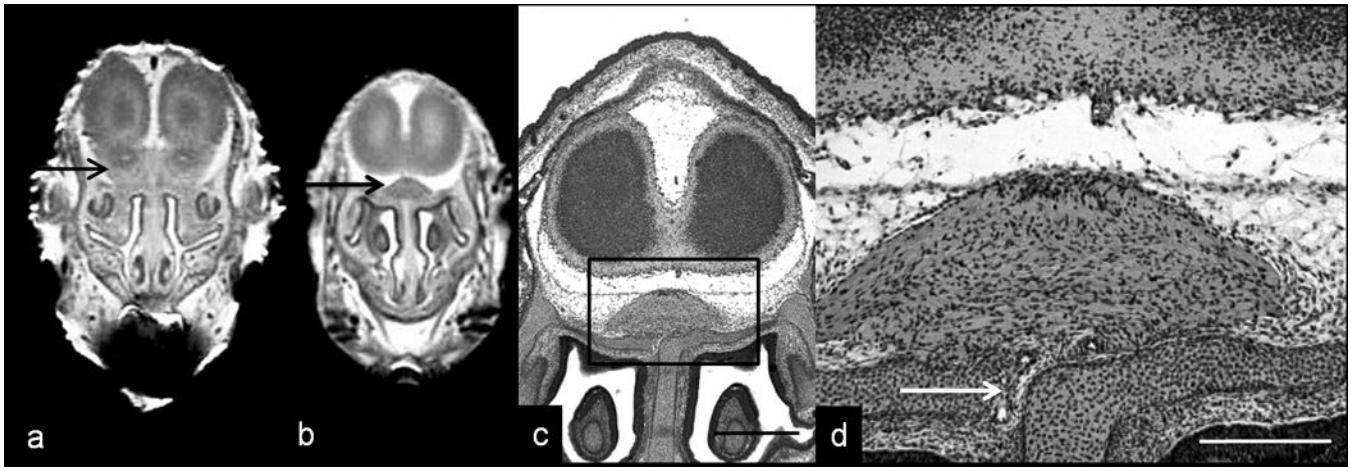

Figure 4.
MRM and routine histology illustrate olfactory nerve abnormality in a holoprosencephalic fetus. As compared to an MRM image of a normal coronal scan (a; arrow indicates olfactory bulb) that from an ethanol-exposed fetus (b; fetus also shown in Fig. 2 d), reveals absence of the olfactory bulbs and the presence of an aberrant intracranial median mass that is located dorsal to the nasal septum (boxed area). Subsequent examination of histological sections through this region revealed that the tissue is continuous, through the cribriform plate, with the nasal epithelium (arrow in d). Bar in c = 0.5 mm, in d = 0.2 mm

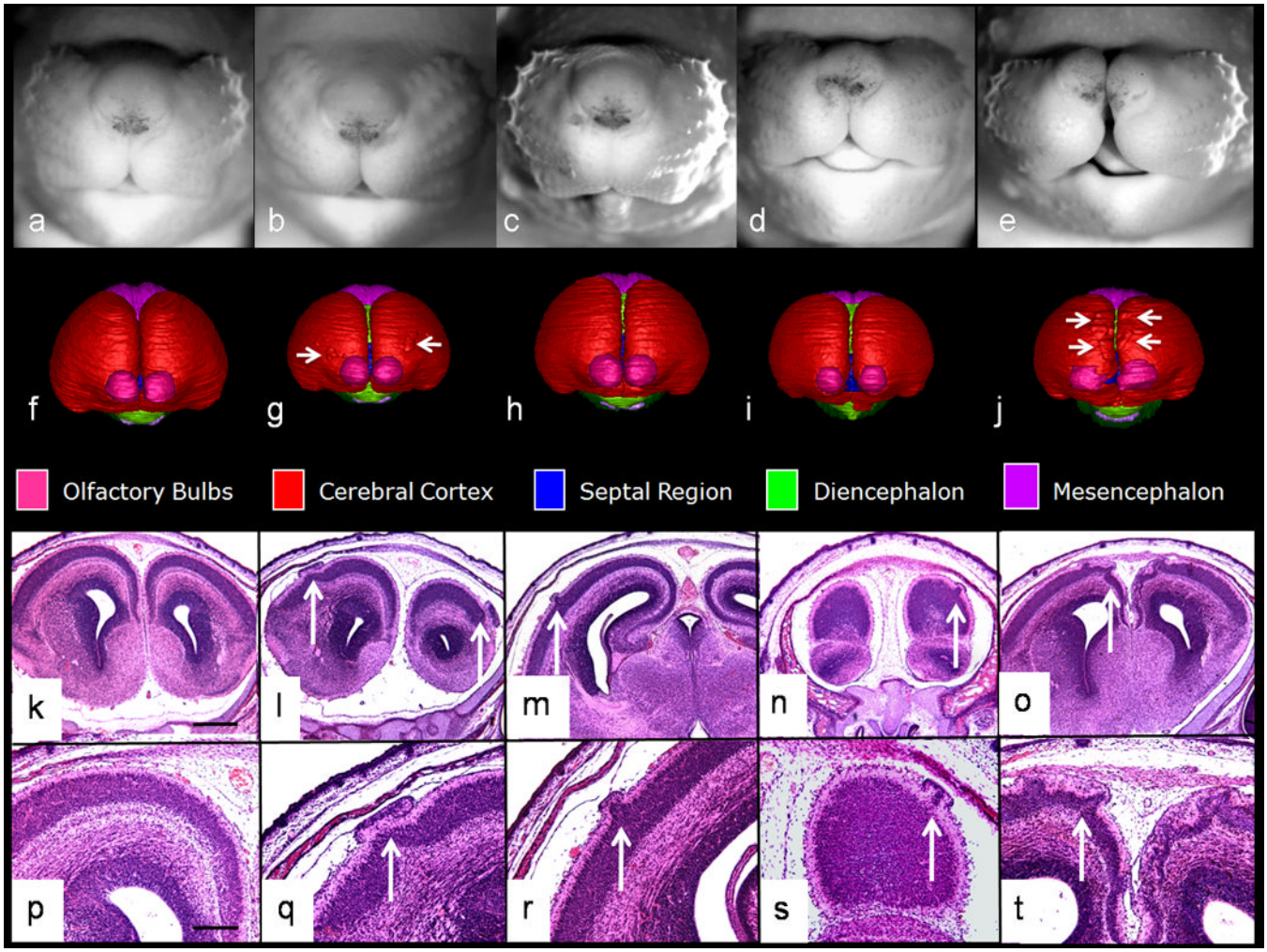

Figure 5.

Shown are the face, brain reconstruction, and histological sections of a control and 4 dysmorphic GD 17 fetal mice. A common feature among the ethanol-exposed animals is cortical dysplasia/heterotopia in the absence of overt HPE. As compared to the control (a), the affected fetuses have faces that appear relatively normal (b), or that present with a long upper lip along with severe micrognathia (c), or foreshortening (d; also note Fig. 6 b) or median cleft of the snout (e). As viewed from the front, reconstructed MRM scans illustrate a slight widening of the space between the cerebral hemispheres (as evidenced by visibility of the septal region and diencephalon) in the affected fetuses (g–j) as compared to control (f). (Color codes for the segmented brain regions are shown beneath the 3D reconstructions.) Also evident in (g) and (j) are irregularities on the cerebral cortical surface (arrows). Subsequent histological analyses of these and the other 2 fetuses shown in this Figure identified these structures as cortical dysplasia/heterotopias (arrows in l–o, 4X; q–t, 10X). Bar in k = 0.5mm, in p = 0.2 mm

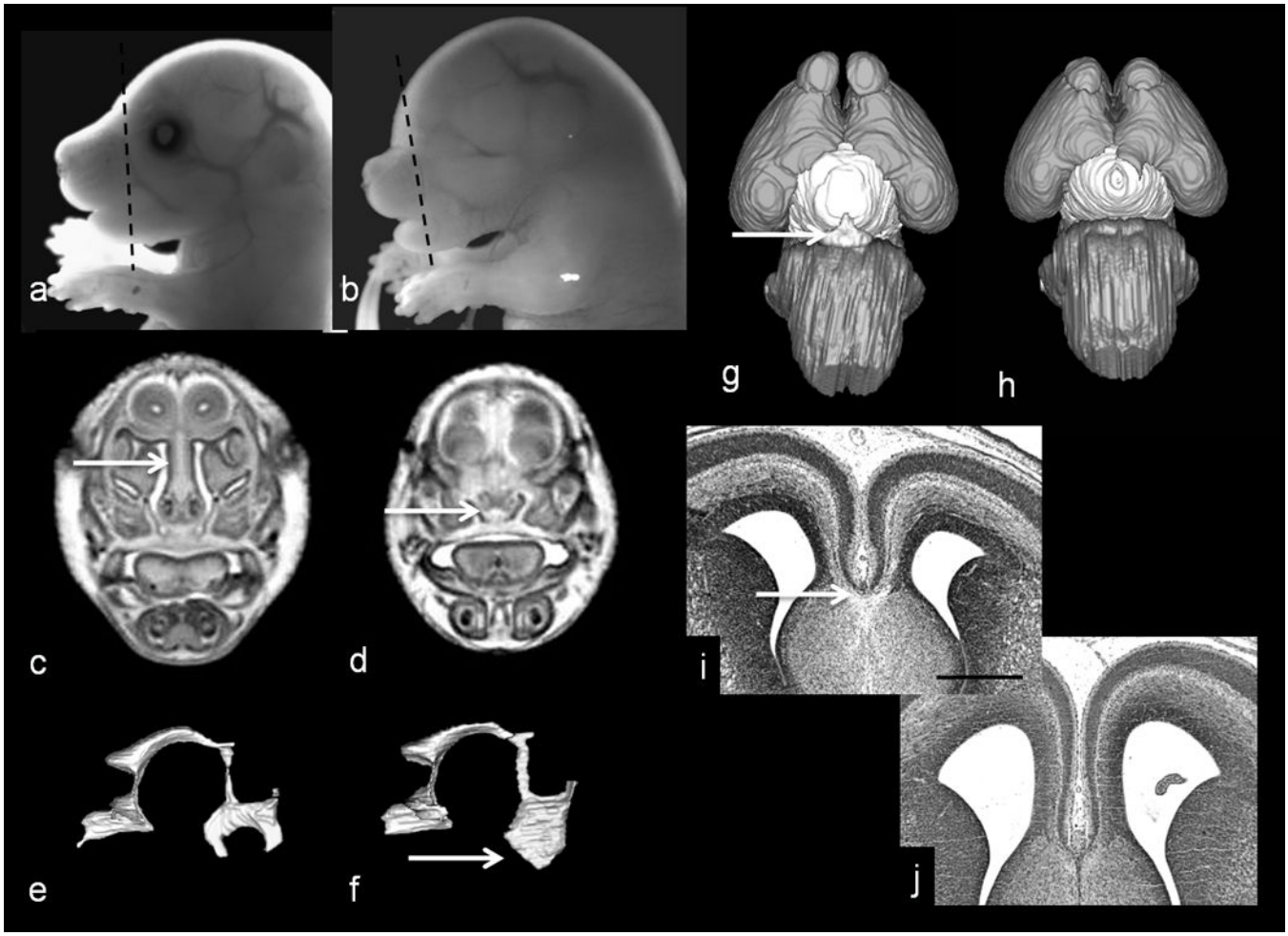

Figure 6.
Additional light micrographs along with coronal MRM scans and reconstructions and histological sections of the fetus pictured in Fig. 5 d illustrate its dysmorphic features as compared to control (a, c, e, g, i) Included are anophthalmia and snout foreshortening (evident in b), short nasal septum and small nasal cavity (arrow in d) [scan made at the level of the line in (b)], third ventricular enlargement (arrow in f), pituitary agenesis (h; compare to control, arrow in g), and apparent absence of the corpus callosum (j; compare to control, arrow in i). Bar in i = 0.5 mm

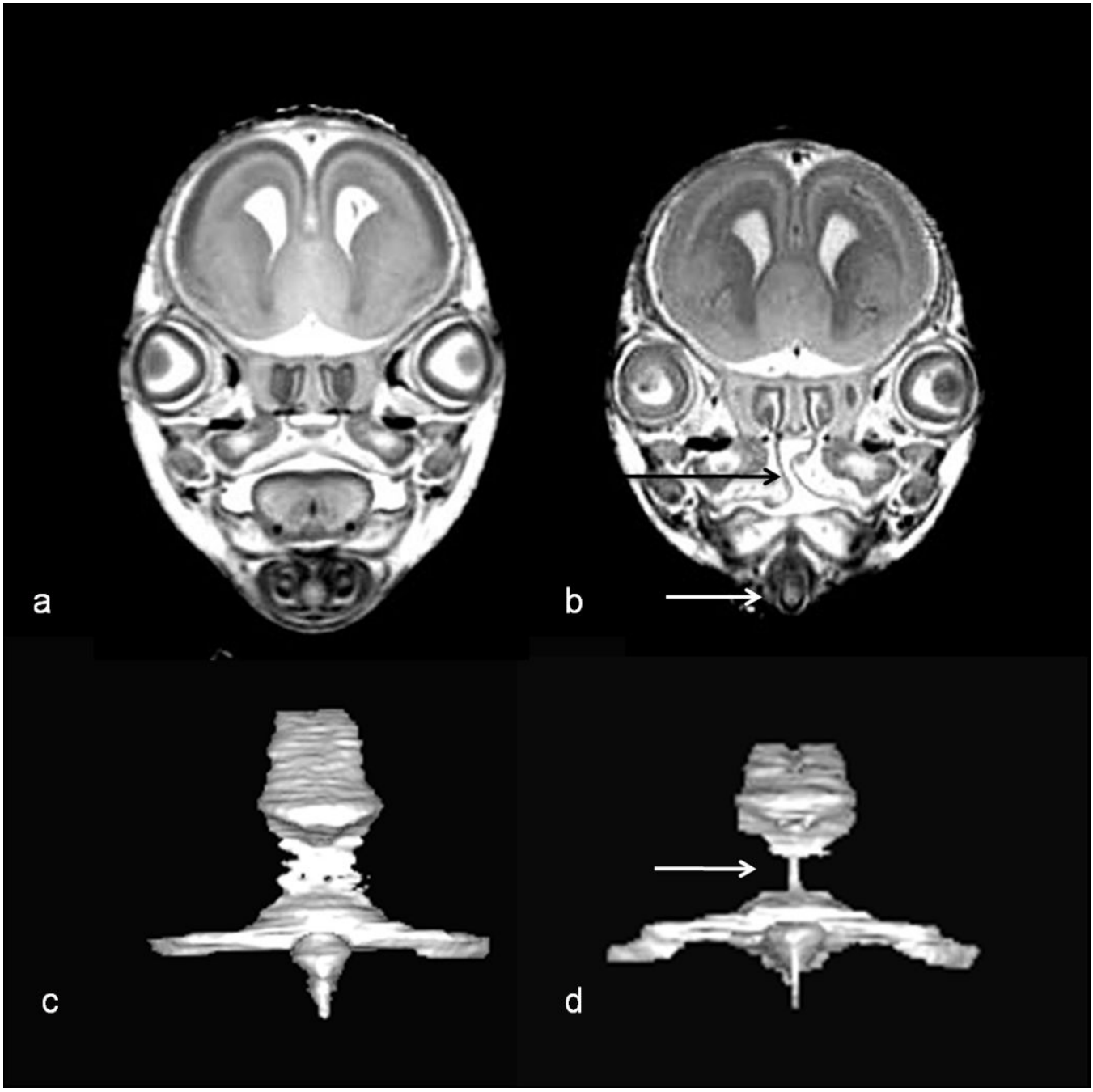

Figure 7.
MRM scans and reconstructions illustrate additional dysmorphic features of the fetus pictured in Fig. 5 c. Coronal scans made at the level of the eyes illustrate clefting of the secondary palate (black arrow in b), no apparent tongue, and this fetus's very narrow mandible (white arrow in b). A posterior view of the reconstructed mesencephalic and fourth ventricle show stenosis (narrowing) at the level of the aqueductal isthmus (arrow in d). Shown in (a & c) are comparable views of a control fetus.

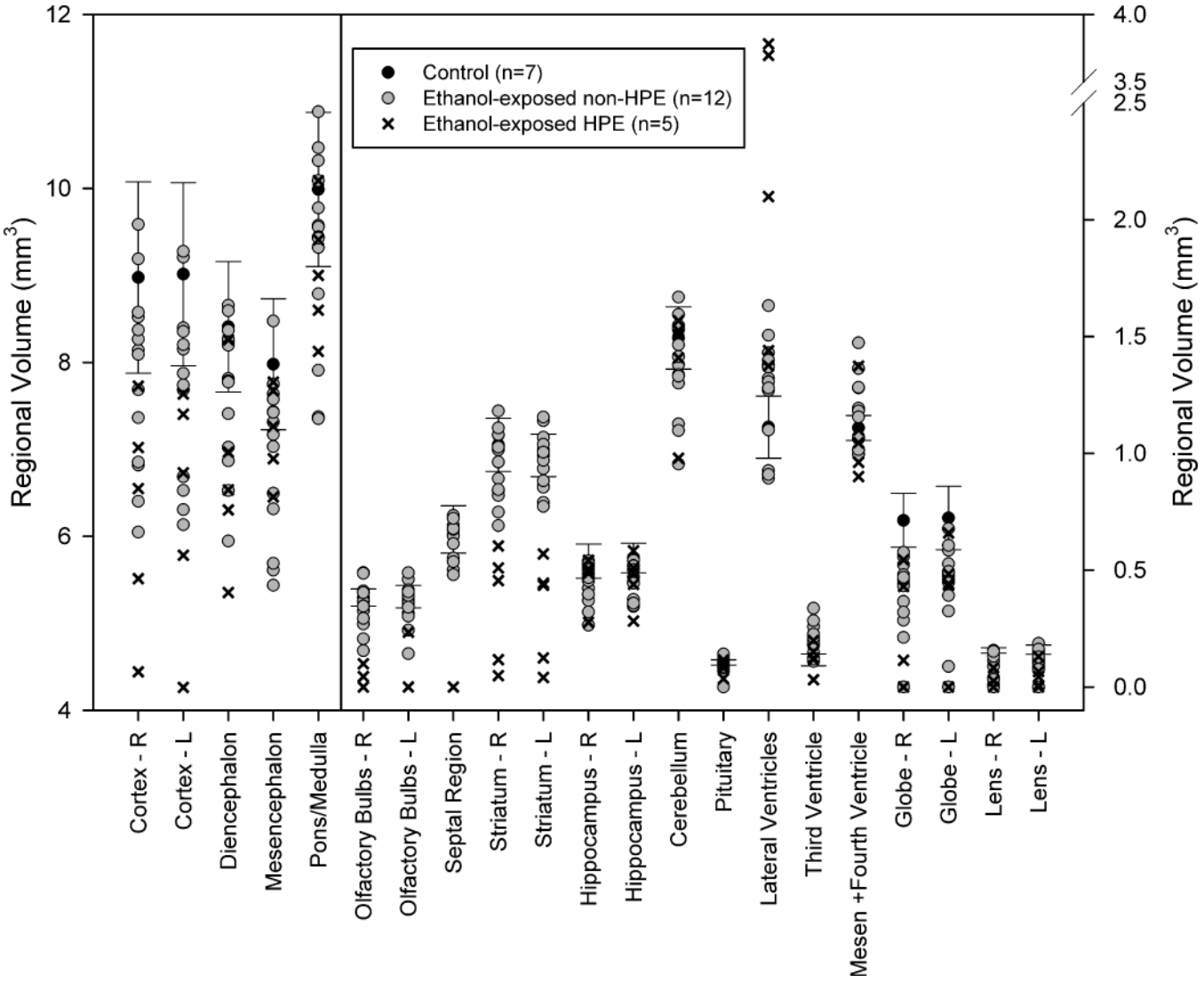

Figure 8.

Ethanol-induces volume changes in selected regions of GD 17 fetal mouse brains following acute GD 7 exposure. Data is expressed to illustrate the broad range of insult. Mean values from 7 control fetuses are indicated by a black dot, with a bar indicating the 95% confidence interval of the control mean. Values for the 5 ethanol-exposed animals with overt HPE are expressed as x's; and for all of the other ethanol-exposed animals (n=14) a grey circle is employed. Please note differing scales on the right and left, as needed to facilitate representation of the data.

Table 1

Linear brain measurements are represented as the mean ± the standard error of the mean. Range of measurements in each region and group are indicated in parentheses.

Mid-sagittal brain length	7.46 ± 0.08 mm (7.21 – 7.84)	7.21 ± 0.99 mm (6.77 – 7.64)	6.75 ± 0.18 mm (6.28 – 7.11)[#, †]
Bulbothalamic distance	3.99 ± 0.06 mm (3.79 – 4.23)	3.78 ± 0.06 mm (3.36 – 4.12)	3.27 ± 0.15 mm (2.90 – 3.60)[#, †]
Third Ventricle Width	0.22 ± 0.02 mm (0.15 – 0.30)	0.23 ± 0.01 mm (0.17 – 0.29)	0.10 ± 0.01 mm (0.08 – 0.13)[#, †]

[#]denotes a significant difference from controls, while

[†]denotes a significant difference from the non-HPE group.

For controls, n=7; non-HPE, n=14; HPE, n=4.